Enhanced utilization of light through polystyrene microspheres for boosting photoelectrochemical hydrogen production in MoS_2/Si heterostructures

Jing Yu,[1, 2] Yingying Wang,[2, a)] Qixiao Gai,[3] Chaoyang Hou,[1] Zhiyong Luan,[4] Yao Liang,[4] Wenjun Liu,[2] and Xiaofeng Fan,[5]

AFFILIATIONS

[1] Department of Physics, Harbin Institute of Technology, Harbin 150001, China

[2] Department of Optoelectronic Science, Harbin Institute of Technology at Weihai, Weihai 264209, China

[3] The College of Basic Department, Information Engineering University, Zhengzhou 450000, China

[4] School of Materials Science and Engineering, Dalian Jiaotong University, Dalian 116028, China

[5] Key Laboratory of Automobile Materials, Ministry of Education, and College of Materials Science and Engineering, Jilin University, Changchun 130012, China

a) Author to whom correspondences should be addressed: yywang@hitwh.edu.cn

EXPERIMENTAL SECTION

1. CVD growth of wafer-scale monolayer MoS_2. In a low-pressure three-temperature zone system, wafer-scale monolayer MoS_2 was synthesized by chemical vapor deposition (CVD). Sulfur (S) powder and molybdenum trioxide (MoO_3) powder served as the reactant precursors, positioned in Zone I and II, respectively. A 1-inch single-side polished sapphire wafer was vertically positioned on the sample holder in Zone III for the deposition of MoS_2. Throughout the growth process, high-purity argon (Ar, 275 sccm) and oxygen (O_2, 3 sccm) were employed as carrier gases, with the system pressure maintained at approximately 0.95 Torr. During the growth, the temperatures in Zones I, II, and III were controlled at 200°C, 580°C, and 900°C, respectively, and maintained for 25 minutes. Notably, the growth sample is subjected to a 5-minute anaerobic annealing treatment to reduce S vacancies.

2. Structure and Composition Characterization. The morphologies of MoS_2 grown on sapphire were initially characterized using Olympus Optical Microscope (OM). Transmission electron microscopy (TEM) was employed to assess the crystal quality characterization of monolayer MoS_2. The thickness of the grown MoS_2 was determined by atomic force microscopy (AFM). X-ray photoelectron spectroscopy (XPS) was utilized to analyze the elemental composition of the grown film. The top view of the polystyrene (PS) microsphere was acquired by scanning electron microscopy (SEM). All Raman spectra were obtained with a 532 nm excitation wavelength as the excitation source.

3. Numerical Simulation: The simulations were performed using COMSOL Multiphysics, based on the finite element method. A 2D cross-sectional model was created to investigate the effects of microsphere MF and WGM on the MoS_2/Si heterostructure. The thickness of MoS_2 was set to 1 nm, consistent with experimental measurements, while the Si layer thickness was set to 1 μm. Periodic boundary conditions were applied to both sides of the model. A plane wave excitation source was used with a periodic port type, activating the slit condition at the internal port, with the slit supported by the domain. The incident wave is an x-polarized plane wave propagating along the -y direction, with an electric field intensity of 1 V/m and an output power of 1 W/m. To simulate the WGMs effect induced by a scatterer, a theoretical simulation was conducted by positioning a dipole moment near the bottom of a 1-μm-diameter PS microsphere. The dipole moment is polarized along the y-axis with a magnitude of 1 A·m.

To assess the MF effects across various sizes, numerical simulations of the electromagnetic field on the Si surface are performed with and without the microspheres. The corresponding ERI_r can be expressed as:[1]

$$ERI_r = 2\pi\int_0^{r_s} |E_s(r)|^2 \, rdr \Big/ 2\pi\int_0^{r_s} |E_0(r)|^2 \, rdr$$

Where E_0 and E_s are the electric field strengths before and after focusing the excitation laser, respectively, and r_s denotes the radius of the optical focusing region on the Si surface.[2] r_s can be written as $r_s = r \cdot \sin(2\theta_{rem} - \theta_{iem})$, here r is the radius of PS microsphere. θ_{rem} and θ_{iem} represent the angles of refraction and incidence on both sides of the interfaces when light enters the microcylinder.[2] The relationship between θ_{rem} and θ_{iem} can be expressed as $\theta_{rem} = \arcsin\left[n_e/n_m\right]\sin(\theta_{iem})]$,[2] here, n_e and n_m represent the refractive indices of the PS microspheres and air, respectively. The refractive index of the PS microspheres varies with different wavelengths. However, upon calculation, the change in the $\sin(2\theta_{rem} - \theta_{iem})$ value is negligible. Therefore, we take the average value of 0.446. As a result, the value of r_s is calculated as 0.446*r*.

4. Electrode preparation

4.1 Preparation of MoS_2/Si electrode: To fabricate the MoS_2/Si electrode, monolayer MoS_2 is transferred onto the Si substrate using the PMMA-assisted wet transfer method.[3] The Si wafer used in this study has a resistivity of 0.01 Ω·cm (p-type, (100) orientation, 625 μm thickness). The wafer was cut into 1 × 1 cm^2 pieces for the preparation of photocathodes. Initially, Polymethyl methacrylate (PMMA) was spin-coated onto the grown monolayer MoS_2 film. The sample was then heated at 60°C for 1 minute and subsequently immersed in a NaOH solution to etch away the sapphire layer, allowing for the separation of the film. Deionized water was used to wash away the etching residues. Next, the suspended film was transferred onto a p-Si substrate that had been etched with 10% HF solution, followed by baking on a hot plate at 60°C for 2 hours to ensure strong adhesion. Finally, acetone was employed to remove the PMMA layer, resulting in a well-attached MoS_2/p-Si heterojunction photocathode structure.

4.2 Preparation of defective monolayer MoS_2/Si electrode: The MoS_2/Si electrode was subjected to oxygen plasma treatment in a plasma processing system. Before plasma treatment, the reaction chamber was evacuated to a base pressure of 2 × 10^{-2} torr to minimize contamination from residual gases. Once the required vacuum level was reached, a 20 sccm argon gas flow was introduced into the chamber. The surface of monolayer MoS_2 was treated by oxygen plasma at the power of 20 W, 30 W, and 40W respectively. The plasma treatment duration is fixed at 10 seconds for the sample.

4.3 Preparation of PS-coupled defective MoS_2/Si (30W) electrode: A homogeneous dispersion was obtained by sonicating a mixture of PS aqueous solution and 10 µL of 0.5 wt% Nafion solution. Subsequently, the solution was spin-coated onto the surface of the MoS_2/Si-30W at 900 rpm for 1 minute. To ensure tight bonding between PS and MoS_2, the electrodes were subsequently vacuum-dried for 6 hours.

5. PEC-HER Measurements. For photoelectrochemical (PEC) hydrogen evolution reaction (HER) measurements, photocathodes were positioned in a standard three-electrode configuration, utilizing an Ag/AgCl rod as the reference electrode and a platinum mesh as the counter electrode. The electrolyte used was an Ar-saturated 0.5 M H_2SO_4 solution. A xenon lamp, calibrated to an output of 100 mW/cm^2 under AM 1.5 G conditions, was employed as the light source. Furthermore, the experimental data were subjected to iR-correction for accuracy.

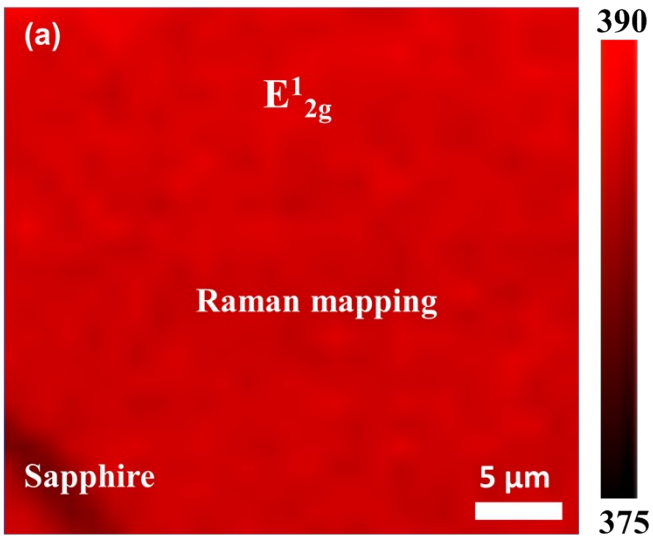

Fig. S1. Raman mapping of the E^1_{2g} peak intensity is conducted on the wafer-scale monolayer MoS_2 with a collected area of 33 µm × 30 µm.

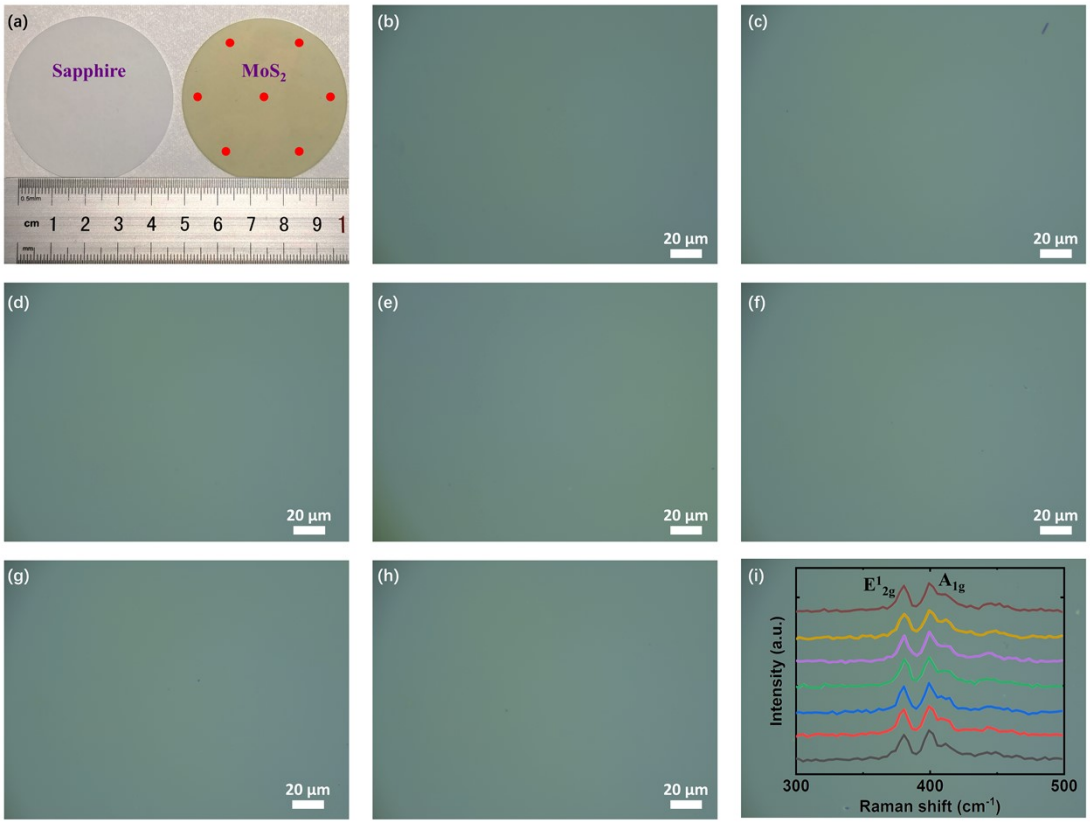

Fig. S2. (a) Photographic image of a bare sapphire substrate and a monolayer MoS_2 directly grown on it. (b)-(h) Optical images extracted from seven random locations on the same wafer in Fig. S2 (a) and corresponding Raman spectra of (i).

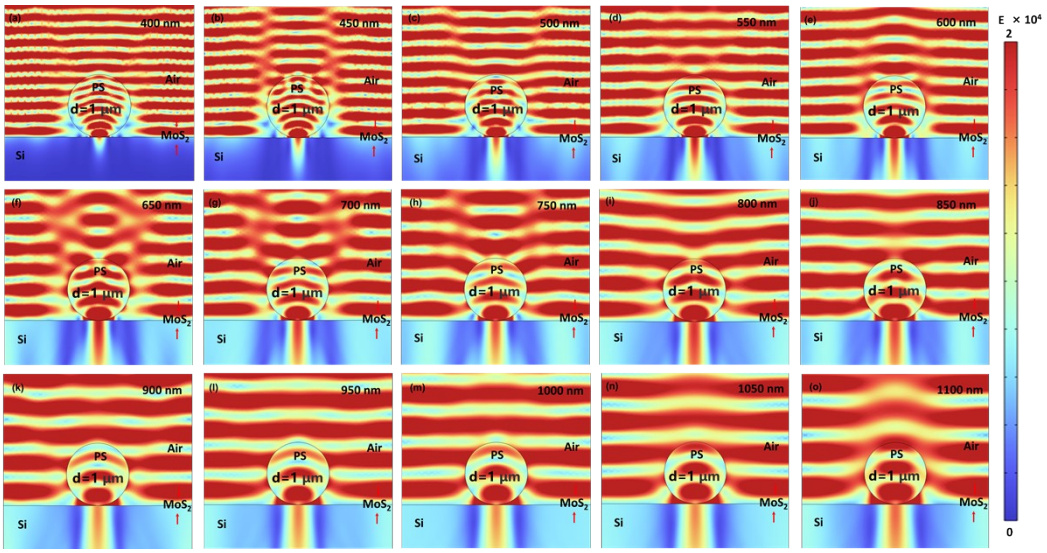

Fig. S3. (a)-(o) Light intensity distribution inside and in the vicinity of 1μm diameter PS microsphere with different wavelengths.

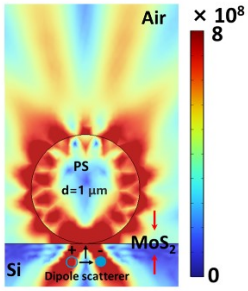

Fig. S4. A typical simulation of whispering gallery modes (WGMs) excited by a dipole scatterer with an emission wavelength of 521.8 nm in free space, positioned near the bottom of a 1-μm-diameter PS microsphere.

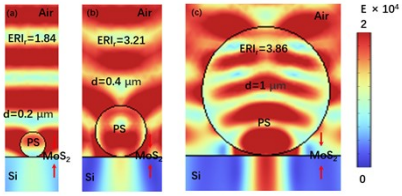

Fig. S5. The electric field distribution of PS-coupled MoS_2/Si structures at the wavelength of 660 nm for various PS diameters: (a) d=0.2 μm, (b) d=0.4 μm, (c) d=1 μm.

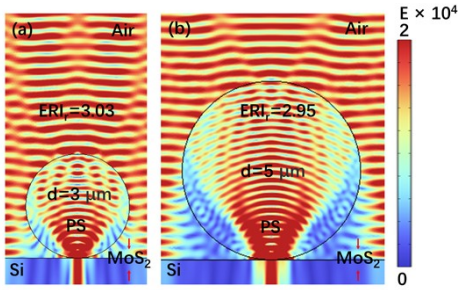

Fig. S6. The electric field distribution of PS-coupled MoS_2/Si structures at the wavelength of 660 nm for various PS diameters: (a) d=3 μm, (b) d=5 μm.

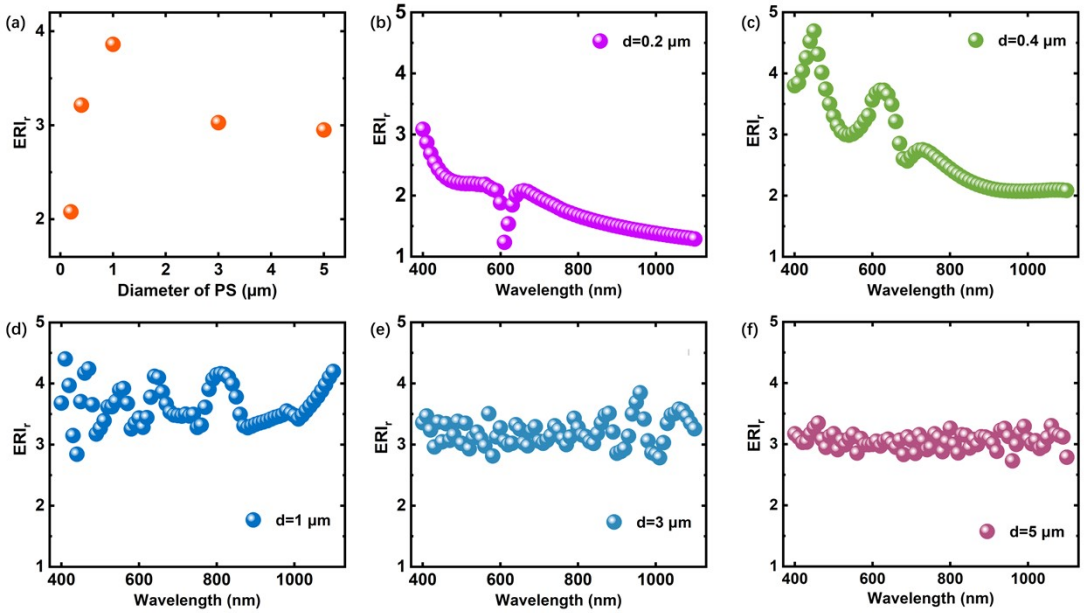

Fig. S7. (a) The calculated ERI results as a function of various PS diameters at a

wavelength of 660 nm. (b)-(f) the corresponding ERI_r values at different wavelengths for PS microspheres with diameters of 0.2, 0.4, 1, 3, and 5 μm.

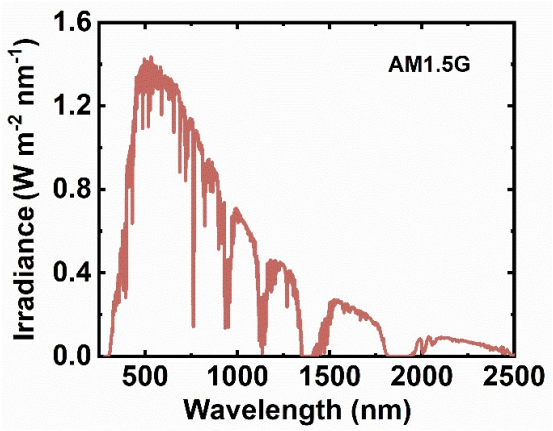

Fig. S8. AM1.5G standard solar spectrum ranges from 250 to 2500 nm.

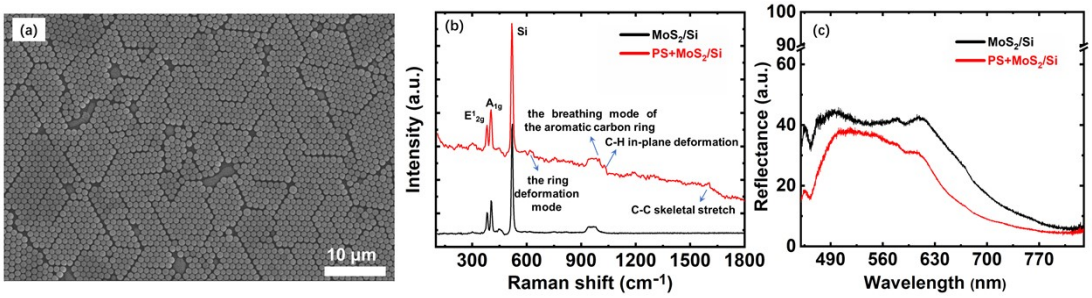

Fig. S9. (a) SEM images of the PS microspheres on MoS_2. (b) Raman spectra before and after the PS-coupled MoS_2/Si structures. (c) Reflectance spectra of MoS_2/Si and PS-coupled MoS_2/Si structures.

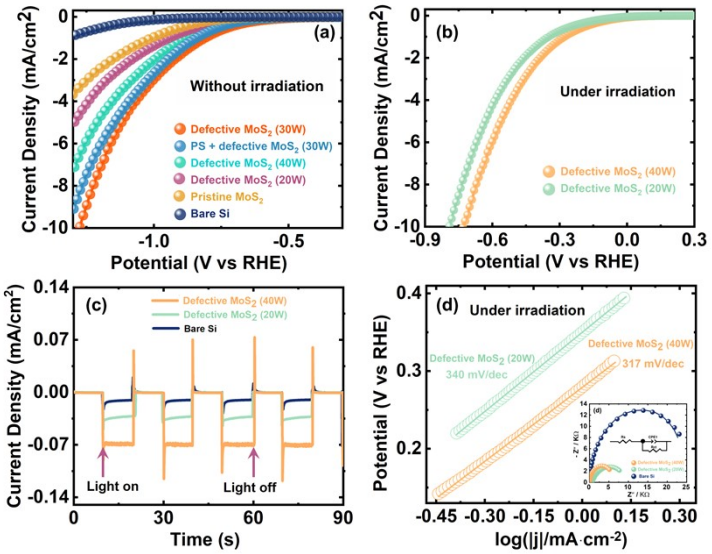

Fig. S10. (a) Polarization curves without irradiation for HER measurements. (b) Polarization curves under irradiation for PEC-HER measurements. (c) Transient photocurrent response of the illuminated on-off cycles at 0 V (vs. RHE) for different samples. (d) Corresponding Tafel plots for the results are given in (b). (d) The inset displays the results of electrochemical impedance spectroscopy (EIS) for the photocathode carried out under irradiation at an overpotential of 0 V (vs. RHE).

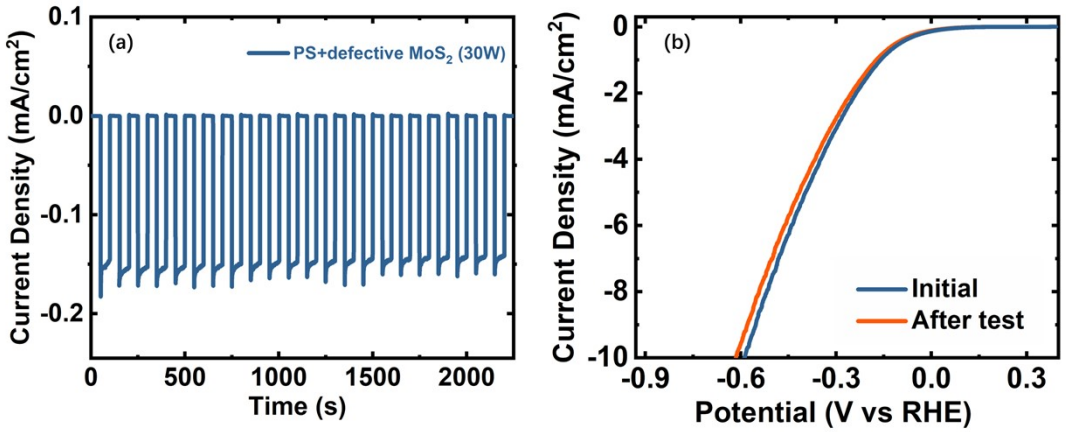

Fig. S11. (a) Photocurrent response of PS-coupled MoS_2/Si (30 W) during the illuminated on-off cycles at 0 V (vs. RHE). (b) LSV curves of PS-coupled MoS_2/Si (30 W) before and after illumination cycles.

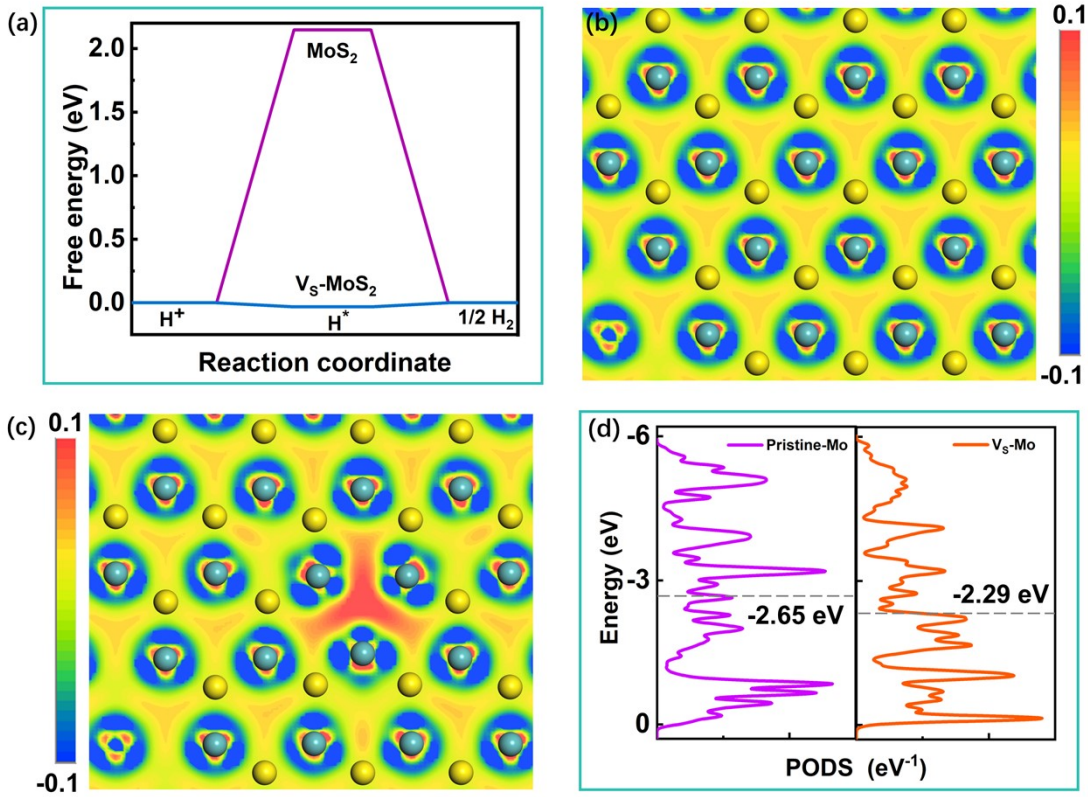

Fig. S12. (a) The ΔG_{H^*} values for pristine MoS_2 and VS-MoS_2, respectively. (b) and (c) Top-view electron density difference maps for pristine MoS_2 and VS-MoS_2, respectively. (d) The projected electronic density of states (PDOS) of the d-band for Mo atoms.

REFERENCES

1. Wang, M.; Yan, Y.; Mi, Y.; Jiang, Y., Flexible Microsphere-Coupled Surface-Enhanced Raman Spectroscopy (Mcsers) by Dielectric Microsphere Cavity Array with Random Plasmonic Nanoparticles. *Journal of Raman Spectroscopy* **2022**, *53*, 1238-1248.

2. Gu, G.; Zhang, P.; Chen, S.; Zhang, Y.; Yang, H., Inflection Point: A Perspective on Photonic

Nanojets. *Photon. Res.* **2021**, *9*, 1157-1171.

3. Yu, J.; Wang, Y.; Liu, W.; Hou, T.; Hao, Y.; Zhong, B.; Wang, X.; Fan, X., Exploring Kinetic Control for the Growth of Layered Mos2(1-X)Se2x Alloy and Its Electrocatalytic Activity in Hydrogen Evolution Reaction. *Applied Surface Science* **2024**, *646*, 158860.